Motion of Particles in A Slider/Disk Interface: Numerical Simulation by Using A Modified Model with Wall Effect Introduced

Shuyu Zhang and David B. Bogy

Computer Mechanics Laboratory

University of California, Berkeley, CA 94720

Abstract

In this report, we studied the motion of particles in a slider/disk interface. A modified model is introduced by considering the wall effect on various forces. Using this model, we did simulation for both small and large particles and found that the results by the new model show similar trends to those without considering the wall effect. That is, the variation of density and initial velocity do not affect the paths of small particles significantly, and these small particles follow the streams very well. For large particles in a recessed region, Saffman lift force shows more significant effect on the motion of particles with larger diameter, density and initial velocities.

1. Introduction

The motion of a particle in an air flow is affected by various forces acting on it. Some of them, such as drag force, shear-induced lift force, etc., will show different values if different boundary conditions are applied. For example, when a particle moves close to a solid wall, the drag force acting on it is actually different from that when it moves far from the wall or in an infinite fluid. So is the shear-induced lift force. The mechanism of this aspect is that the existing solid wall causes an additional disturbance in the flows.

Wall effects were considered by several researchers in their studies on the motion of particles in a fluid. Kallio (1989) studied the particle motion through the boundary layer of a turbulent gas. In his model, the drag, shear-induced lift and gravity force are involved for predicting the motion of particles. The drag coefficient in it is calculated by using the Stoke's drag law multiplied by molecular slip correction, wall effect correction and fluid inertia effect correction. The results show that the shear-induced lift significantly affects particle impact in the turbulent boundary layer, while the increase in drag due to the wall plays a relatively minor role unless the particle is very close to the wall. Chen and McLaughlin (1995) studied numerically the deposition rate of particles in a turbulent flow inside a vertical duct. In their model, the motion of the particles is governed by the modified Maxey-Riley equation which includes the drag force, the shear-induced lift force, and the Bronian random force, and the wall effect is considered in both drag and shear-induced lift. Their model is about the particle motion in a duct with two parallel planes, but they apply the wall effect corrections obtained from the particle motion related to a single plane because they argue that the dimension between the two planes is much larger than the dimension of the region in which the wall effects will play a significant role.

A particle moving in an air bearing or a recessed region can be regarded as moving in an air flow within two parallel planes. In our previous study (Zhang and Bogy, 1996), we assume that the particle is very small so the wall effects are neglected in the simulation. In this report, we will introduce wall effects into the model and see how they will influence the motion of particles close to a wall. For convenience, we use "interface" to denote both air bearing and recessed regions in the following analysis, unless they are specially mentioned.

2. Model

The particle motion equations can be expressed as follows:

$$\frac{d\mathbf{x}_p}{dt} = \mathbf{v}_p , \tag{1}$$

$$m_p \frac{d\mathbf{v}_p}{dt} = \mathbf{f}_d + \mathbf{f}_s + \mathbf{f}_g , \tag{2}$$

where m_p is the mass of the particle (for simplification, we assume the particle is a sphere), t is the time variable, $\mathbf{x}_p$ and $\mathbf{v}_p$ are position and velocity vectors of the particle in the air flow of interface, $\mathbf{f}_d$, $\mathbf{f}_s$, and $\mathbf{f}_g$ are, respectively, the drag, Saffman lift, and gravity force acting on the particle. Since the Magnus lift is much smaller than the other forces (Zhang and Bogy, 1996), it is not considered in this report.

The drag force, with wall effects considered, can be expressed as:

$$\mathbf{f}_d = \frac{\pi}{8} C_d C_w \rho_g d^2 \left|\mathbf{v}_g - \mathbf{v}_p\right| \left(\mathbf{v}_g - \mathbf{v}_p\right) \tag{3}$$

where C_d is the drag coefficient; C_w is the coefficient of the wall effects correction; d is the diameter of the sphere; ρ_g is the density of the air; $\mathbf{v}_g$ is the velocity in air phase. In this report, we use Liu, *et al's* results (1965) to calculate drag coefficient, which is expressed as:

$$C_d = C_{dfm}\left[1 - \frac{B(S)}{Kn_d}\right] \tag{4-a}$$

$$C_{dfm} = \frac{2}{S^3}\left[\frac{4S^4 + 4S^2 - 1}{4S} erf(S) + \frac{e^{-s^2/2}}{\sqrt{\pi}}\left(S^2 + \frac{1}{2}\right)\right] + \frac{2}{3}\frac{\sqrt{\pi}}{S}\sqrt{\frac{T_w}{T_\infty}} \tag{4-b}$$

where the speed ratio $S = |\mathbf{v}_g - \mathbf{v}_p| / (2RT_\infty)^{1/2}$; the Knudsen number $Kn_d = \lambda/d$, and λ is the mean free path of the air; $B(S)$ is a function of speed ratio S (Liu, *et al*, 1965); C_{dfm} is the free molecular drag of the sphere (Schaaf, *et al*, 1961).

Wall effect coefficient C_w appears in different forms for particles moving parallel or vertical to the wall. For particles moving parallel to a single wall, Chen and McLaughlin (1995) calculated the C_w by applying Goldman *et al* (1967), O'Neill (1964) and Faxen's (1923) results, respectively, for the three different regions based on the distances of particles from the wall. That is, applying Goldman *et al*'s for $\delta/a < 0.01$, O'Neill's result for $0.01 < \delta/a < 10$, and Faxen's result for $\delta/a > 10$. Here, $\delta = l_w - a$, and l_w and a are respectively the distance of the particle center to the wall and the radius of the particle. Wakiya (1957) calculated the drag force for viscous flow past a spheroid between two parallel plane walls. For a spherical particle located at the place away from one plane by one-quarter of the distance between the two planes, Wakiya obtained C_w for Poiseuille flow and Couette flow respectively. A comparison between Chen *et al* [1] and Wakiya's results is shown in Fig. 1.

It is seen that when $a/l_w < 0.8$, there is no much difference for C_w among the three results. When $a/l_w > 0.8$, Chen *et al* 's result becomes much larger than Wakiya's results for both Poiseuille and Couette flows and tends to infinite when $a/l_w \to 1$. This is hard to be accepted for a particle moving within the mfp distance to the wall in a rarefied gas flow. Since our study is

[1] It is actually Goldman *et al*, O'Neill and Faxen's results. Here we use Chen *et al* to represent them for convenience.

focused on the particles moving in a rarefied gas flow, we assume that C_w is finite when particles close to the wall. Therefore, Wakiya's results looks more reasonable.

For $a/l_w < 0.8$, we already know that C_w does not change very much from one plane wall case (Chen *et al*'s result) to two plane wall cases (Wakiya's results). For $a/l_w > 0.8$, we assume that Wakiya's results are better approximations to C_w for particles moving close to the wall. Since particles in which we are interested are very small, the velocity field near them can be regarded as linear. Therefore, Wakiya's result for Coutte flow is adopted in this report, which can be expressed as:

$$C_{wx} = C_{wy} = \frac{1}{1 - 0.6526\left(a / l_w\right) + 0.4003\left(a / l_w\right)^3 - 0.297\left(a / l_w\right)^4}, \qquad (5)$$

where, subscripts *x* and *y* represent the correction for *x* and *y* moving directions, and lw is taken as the smaller distance of a particle away from the walls.

For a sphere moving perpendicularly towards a solid plane wall, Brenner (1961) obtained a correction to the Stoke's Law by solving the creeping motion equations. A characteristics for this result is that the value of the correction tends to be infinite when the sphere moves close to the wall. A reason for this result is that Brenner used a continuos model to solve the problem. Chen and McLaughlin (1995) argued that the Van der Valss force become important when the sphere moves within a distance shorter than the *mfp* of the air to the wall. As a simplified treatment, they assumed that the contact occurred when the sphere is within the *mfp* distance away the wall.

In our report, we use Wakiya's result (1960) for a sphere moving towards to a solid plane wall. This result agrees very closely with Brenner's result for $a/l_w < 0.1$. When the sphere moves close to the wall, Wakiya's result shows a finite value for the correction instead of a infinite value as Brenner's result. Wakiya's wall correction is expressed as:

$$C_{wz} = \frac{1}{1 - 1.125(a / l_w) + 0.5(a / l_w)^3}, \tag{6}$$

where, subscript *z* represents the motion in *z* direction.

McLaughlin (1993) presented a solution for the lift force acting on a small rigid sphere that moves parallel to a flat wall in a linear shear. This lift force can be expressed as:

$$f_s = \frac{9}{\pi} J \mu_g a^2 \Delta U \left(\frac{G}{\nu_g} \right)^{1/2}, \tag{7-a}$$

where μ_g and ν_g are the viscosity and kinematics viscosity of the air; ΔU is the velocity of the sphere relative to the air flow; *G* is the magnitude of the velocity gradient; *J* is an integral coefficient. For a sphere sufficient far from the wall ($l_w \to \infty$), *J* converges to the Saffman's value, that is, $J \to 2.255$. When the sphere close to the wall, *J* will take different values depending on the ratio of $\varepsilon = (Re_G)^{1/2}/Re_s$ and a non-dimensional distance $l_w^* = (G/\nu_g)^{1/2} l_w$. Here, $Re_s = \Delta U a / \nu_g$ and $Re_G = G a^2 / \nu_g$. For sufficient large ε and $l_w^* < 1$, the value of *J* by McLaughlin reduces to the result obtained by Cox and Hsu (1977), which can be expressed as:

$$J = \frac{\pi^2}{16} \left(\frac{1}{\varepsilon} + \frac{11}{6} l_w^* \right). \tag{7-b}$$

For the air flow in a recessed region, the thickness dimension is usually several micro-meters, and the relative velocity ΔU is of the magnitude of $0.1\hat{U}$. The diameter of the sphere in which we are interested is around 200 *nm*. Thus, $Re_s \sim 0.01$ and $Re_G \sim \hat{U} a^2 / h \nu_g \sim 0.01$ which leads to $\varepsilon \sim 10$, and $l_w^* \sim 1$ or less. Therefore, equation (7-b) is valid for the cases in our study and adopted in this report.

The gravity force is expressed as:

$$f_g = \frac{4}{3}\pi a^3\left(\rho_g - \rho_p\right)g_z \tag{8}$$

where g_z is the component of the gravity acceleration in the z direction. In (8), the buoyancy is involved although it is negligible compared to the gravity force.

We have analyzed and given explicitly all the forces appearing in (2). Substituting them into (2) and rearranging results in a non-dimensional form, we obtain the following component expressions for the motion equations for a sphere:

$$\frac{dX_p}{dT} = R_l U_p\,, \tag{9-a}$$

$$\frac{dY_p}{dT} = R_l V_p\,, \tag{9-b}$$

$$\frac{dZ_p}{dT} = R_h W_p\,, \tag{9-c}$$

$$\frac{dU_p}{dT} = \frac{3}{4}R_h\frac{\rho_g}{\rho_p}\frac{C_d C_{wx}}{D}\overline{U}\left(U_g - U_p\right), \tag{9-d}$$

$$\frac{dV_p}{dT} = \frac{3}{4}R_h\frac{\rho_g}{\rho_p}\frac{C_d C_{wy}}{D}\overline{U}\left(V_g - V_p\right), \tag{9-e}$$

$$\frac{dW_p}{dT} = \frac{3}{4}R_h\frac{\rho_g}{\rho_p}\frac{C_d C_{wz}}{D}\overline{U}\left(W_g - W_p\right) + \frac{27}{32}\left(\frac{1}{\varepsilon} + \frac{11}{6}l_w^*\right)R_h Re_h^{-1/2}\frac{\rho_g}{\rho_p}\frac{\tilde{U}}{D}G^{1/2} + R_h\left(\frac{\rho_g}{\rho_p} - 1\right)\frac{h_m}{\hat{U}}g_z \tag{9-f}$$

where, $X=x/l$, $Y=y/l$, $Z=z/h_m$ are non-dimensional position variables, l is the length of the slider and h_m the initially given height of the air bearing at the trailing edge; $U = u/\hat{U}$,$V = v/\hat{U}$ and $W = w/\hat{U}$ are non-dimensional velocity components; non-dimensional time $T = \hat{\Omega}t$, and $\hat{\Omega}$ is the rotation speed of the disk; $\overline{U} = [(U_g\text{-}U_p)^2 + (V_g\text{-}V_p)^2 + (W_g\text{-}W_p)^2]^{1/2}$ and $\tilde{U} = \Delta U / \hat{U}$ are non-

dimensional velocities; non-dimensional diameter $D = d/h_m$; non-dimensional numbers $R_l = \hat{U} / \hat{\Omega} l$, $R_h = \hat{U} / \hat{\Omega} h_m$, and Reynolds number $Re_h = \hat{U} h_m / \nu_g$.

Velocity field of the air flow is obtained by solving the Reynolds equation by the finite difference and multi-grid control volume methods. To solve the particle transport equations, we use the classical Runge-Kutta method. The detailed information about these methods can be found in related documents (Partanka, 1980; Shyy *et al* 1993; Cha *et al* 1995; Lu *et al* 1994 and 1995; Zhang *et al*, 1996).

3. Anti-contamination Slider Designs

In this section, we first study the characteristics of small particles moving in an interface and compare the results with cases without considering the wall effect (Zhang and Bogy, 1996b). Based on the study results, we present some experiences in slider designs for controlling particle contamination, and then introduce a slider which is regarded as good for reducing the contamination. Since we are only interested in the small particles which can move in an air bearing with thickness less than 100 *nm*, we can ignore the lift and gravity forces in the model because these forces have few effects on the motion of the small particles with $d < 100$ *nm*. This fact can be seen in the discussion in next section. Thus, the motion of small particles can be simplified as a planar one, and the equations involving the lift and gravity forces can be taken off the model for this special case. That is, only equations (8-a, b, c, d) are used in the analysis.

In calculating the coefficient of wall effect, we take l_w to be the half thickness of the air bearing because the particles can be approximated as moving at the medial position of it. For the convenience of data analysis, 50% type sliders with load of 3.5*g* are chosen. The tapers for all

simulated sliders have the same angle and length, 0.01 *rad* and 0.2 *mm*, and a recession height of 3 μm. Except for some specially denoted cases, all sliders are assumed to fly at the position r=23 *mm* away from the center of the disks while the disks rotate at 5400 *rpm*. For a demonstration, a slider (#1) shown as in Fig.2(a) is simulated and the results are shown Table 1 and Fig. 2 (b).

Table 1 shows the flying characteristics of the slider. It is seen that the flying height at the central trailing edge (FH-CTE) is 34.2 *nm*. Figure 2 (b) shows the paths of particles moving in the interface. In this case, seven particles, each with diameter d = 30 *nm*, density ρ_p = 4000 kg/m^3 and initial velocities $U_0 = \hat{U}$ and $V_0 = 0$, are evenly spaced at the leading edge. For the convenience of analysis, particle paths are drawn in wide lines to be distinguished from thin lines that represent the "stream lines" of the air flow. Here, the "stream lines" are drawn based on the average flux in the interface (averaged across the thickness of the interface), and drags on particles are calculated based on the average velocity in the same sense. Note that the air flow in the interface can be approximated as a plane flow, that is, the z component of velocity is constant (approximately zero), while the x and y components of it vary in the z direction. Therefore, the drag on a particle is actually different at different z positions. Fortunately, the thickness of the interface is much smaller than the x and y dimensions of it and close to the size of the particle studied, therefore, the employment of the average velocity will not bring significant errors in the simulation, at least for those particles moving in the air bearing, and those moving in the recessed region but not closely adjacent to the slider and disk surfaces.

(1) Effects of the particle density on the motion of particles

In this case, we choose the same slider shown as in Fig. 2(a). To study the effects of the density, we consider these quite different values: ρ_p=1000, 3000, 6000 and 8000 kg/m^3. The diameter of the particle is chosen to be 30 *nm* , and the initial velocities $U_0 = \hat{U}$ and $V_0 = 0$.

Again, seven particles are evenly spaced at the leading edge. The simulation results are shown in Fig. 3. It is seen that the particle paths changes very slightly with the variation of the particle densities (Fig. 3(a)). To see the changes clearly, we apply a smaller scale to plot the paths of particles with ρ_p=1000 and 8000 kg/m^3 and start from the central leading edge in Fig. 3(b). Obviously, only when the particles reach the central rail at the trailing edge do the paths depart an observable amount. This fact implies that the density does not influence the particle motion significantly if the particle size is fine and the density varies in a practical range. This conclusion is same as the case without considering the wall effect (Zhang and Bogy, 1996b).

(2) Effects of the initial velocities

To study the effects of the initial velocities of particles, we choose (U_0, V_0) = (1, -1), (1, 1), (0, -1), (0, 1), respectively, for particles with same density ρ_p = 8000 kg/m^3 and same size d = 30 nm. Again, seven particles are evenly spaced along the leading edge. The simulation results are shown in Fig. 4. It is seen that, like the case in changing density, the variation of initial velocities affects the particle motion very slightly (Fig. 4(a)). Fig. 4(b) shows the paths by using a smaller scale for two particles starting from the central leading edge with initial velocities, respectively, (U_0, V_0) = (1, -1) and (0, 1) (Fig. 4(b)). Obviously, the variation of initial velocities does not significantly change the particle paths even for the particles have big difference in U_0 and V_0. This conclusion is also same as that without considering the wall effect (Zhang and Bogy, 1996(b)).

(3) Effects of particle sizes

At the beginning of this section, we mentioned that we would focus our studies on small particles (say 30 nm) because we are only interested in particles that can go through the air bearing. However, for some special cases, for instance those particles moving in the recessed

regions, it is desirable to consider larger particles. Using the same slider and flying characteristics as in 3(1) and (2), we studied how larger particles move through a recessed region. We do not treat the effects of collisions of the particle with the surfaces of the slider. Therefore, the calculation is stopped when the particle hits the rails.

Figure 5(a) ~ (b) show the effects of density under different particle sizes. In Fig. 5(a), particle diameter is chosen to be d = 30 *nm* and initial velocity to be U_0 = 1, V_0 = 0. It is seen that the paths of particles with ρ_p = 1000 and 8000 kg/m^3, respectively, show little difference under this diameter d. In Fig. 5(b), we change the particle diameter to be d = 300 *nm* and keep the same initial velocities. In this case, the particle paths for ρ_p = 1000 and 8000 kg/m^3 show obvious difference compared to the case with d = 30 *nm*. This implies that the inertia will play more significant role in the particle motion for larger particles. The similar results can be seen for changing the initial velocities under different particle sizes (Fig. 5(c) and (d)).

Figure 5(c) and (d) show the results for d = 30 and 300 *nm*, respectively. Under each particle size, two initial velocities are used, that is, (U_0 , V_0) = (1, -1) and (0, 1). The density ρ_p = 8000 kg/m^3 for both cases. Obviously, the paths of particles show little difference for different U_0 and V_0 under d = 30 *nm* (Fig. 5(c)). But for d = 300 *nm*, their paths show significant difference for different U_0 and V_0. Therefore, the variation of the initial velocities will have an important effects on the particle motion for large particles. This conclusion is similar to that without considering the wall effect.

It should be mentioned that lift forces affect the particle motion significantly for large particles. But for the particles with d < 300 *nm* as in this section, neglecting the lift forces can be regarded as a rational approximation in the analysis.

(4) Slider designs for controlling particle contamination

From the above discussions, we know that the density and initial velocities have little effects on the motion of small particles in an interface, and they follow the streams very well. These suggest that if we can find designs that make more air flow out of the interface from sides of it, we can also make more particles flow out of the interface from sides of it, simultaneously. Based on this concept, we designed a new slider (#2) shown as in Fig. 6 (a). Its rail shape, with a sharp head for the end rail at the central trailing edge, is a little different from that of the slider (#1) as in Fig. 2(a). This modification will make the flow better for particles to pass by the end rail.

Table 2 shows the flying characteristics of the slider #2 for the same given conditions as for the slider #1. Based on these results, the motion of particles is simulated and the results are shown in Fig. 6(b). Seven particles, all having the same diameter of d=30 *nm* and density of ρ_p=4000 kg/m^3, are evenly spaced along the leading edge. The initial velocities for these particles are given by U_0 = 1 and V_0 = 0. Since the particles may enter the interface from the two sides when the slider moves radially over the disk, we also put seven particles at each side and give them a non-zero V_0, that is, U_0 = 1 and V_0 = 0.5 for those from the inner side, and U_0 = 1 and V_0 = -0.5 for those from the outer side.

Obviously, most of particles entering the interface from the leading edge leave the interface from the two sides. The particles starting from the two sides have less chances to go a long distance in the interface. The particle from the central leading edge go through the interface and leave the trailing edge by passing the end rail there instead of going through the air bearing under it as in Fig. 2(b). This demonstrates the advantage of the modified slider.

(5) Effects for slider at ID and OD

We know that small particles follow the streams very well. If the flow field changes, for instance when sliders moves from OD to ID, how will the motion of particles be affected? To

study the effects, we examine two cases for the slider #2 at ID with r = 15 *mm* and skew = -7.5° and OD with r = 31 *mm* and skew = 7.5°. Here, the minus sign corresponds to the case that the flow comes from the outer leading edge towards the inner trailing edge. The flying characteristics for the two cases are shown in Table 3.

For both cases, all the conditions for particles are same as in 3-(4) except for the particle size which we take d = 20 *nm* for ID case and 30 *nm* for OD case because we hope the particle size should be consistent to the flying height at the central trailing edge (Table 2). The simulation results are shown in Fig. 7(a) and (b). For both cases, obviously, most of particles from the leading edge leave the interface from the two sides, which is qualitatively the same as the case for skew = 0. For particles from the inner or outer sides, two more particles, compared with the case of skew=0 in Fig. 2(b), enter the interface from positions close to the trailing edge. Since these two particles travel a short distance through the recessed region at the end corners, they have less chance to deposit on the end rail than those that enter the interface from the leading edge and leave from the trailing edge through or close to the air bearing under the end rail. Therefore, for ID and OD cases, slider #2 still keep the advantage for reducing particle contamination.

From above analysis, we find that the simulation results by considering the wall effects are similar to that without considering the wall effects. The reason for it is because the introduction of the wall effect usually increases the drag force acting on the particles, which causes the motion of particles shows less inertia effect than that without considering the wall effect. In other words, the simulation results with wall effect introduced should make particles follow the streams closer. Therefore, the concept of designing anti-contamination slider in our previous work (Zhang and Bogy, 1996(b)) is still applicable here.

4. Effects of Lift Force on Particle Motion

We mentioned in the last section that lift forces had significant effects on the motion of large particles. The case often occurs when a large particle get into a recessed region, which will be studied in this section. Since we are only interested in the motion characteristics of the particles, we can consider a simple slider which causes a simple flow close to that in a recessed region of a real slider. For convenience, we adopt an "infinitely wide, no-rail slider" with some parameters fixed close to those of a recessed region, for example, with h_m =3.05μm, l=2.05 mm, pitch angle=150 μrad. Here, to take h_m =3.05μm is because the recessed height is usually about 3 μm for a real slider, and 50 nm is a typical value of the minimum spacing under the rails.

(1) Effects of particle size

In this case, we simulate four particles with the same density of ρ_p =8000 kg/m_3 and different diameters of 200 nm, 300 nm, 330 nm, and 340 nm respectively. All of them enter the recessed region with initial velocity of U_0 =1 and initial vertical position of Z_0=0.2. The simulation results are shown in Fig. 8.

It is seen that all four particles go up when they enter the recessed region because their initial velocities are higher than that of the air flow. The particle with d = 200 nm only rises a small distance and then goes almost parallel to the disk surface, while the particle with d = 340 nm goes up sharply and hits the surface of the slider. This implies that the Saffman lift force has more significant effect on the larger particles, which is similar as the case without considering the wall effects (Zhang and Bogy, 1996). Since the existence of wall increases the drag force and

reduces the Saffman lift force, particles usually rise shorter distances in this case compared with the particle of the same size in the case without introducing the wall effects.

(2) Effects of the relative velocities

According to Saffman's analysis, relative velocity of the particle (velocity relative to the local air flow) affects the lift force not only in direction, but also in magnitude. In this case, we simulate particles with the same density of $\rho_p = 8000\ kg/m^3$ and diameter $d = 340\ nm$, but different initial velocities of $U_0 = 0.2$, 0.4, 0.6 and 0.8, which implies different initial relative velocities. The simulation results are shown in Fig. 9.

It is seen that the particle with high (or low) initial velocity, or large magnitude of relative velocity, goes up (or down) sharply when it enters the recessed region. The larger the magnitude of the relative velocity, the more sharply the particle moves up or down. These results are same as the case without considering the wall effects except for that larger relative velocity is required for the Saffman lift force to make considerable effect on the motion of particles if considering the wall effect.

(3) Effects of the particle density

To study the effects of the particle density, we simulate particles with densities of, respectively, 2000, 4000, 6000 and 8000 kg/m^3. All of them have the same diameter of 340 *nm*, and enter the recessed region with initial velocity of $U_0 = 1$ and initial height of $Z_0 = 0.2$. The simulation result is shown in Fig. 10.

It is seen that particles goes up more sharply for those with higher density, or, the Saffman lift force affects the motion of particles with higher density more significantly. The reason for this is that the drag force affects less on the motion of heavier particles so they can move a longer time with large relative velocity. This fact can be checked mathematically by dividing the drag terms

in eq. (9-d, e, f) by 3 and simulated the case with the same given conditions as above. The simulation result is shown in Fig. 11.

It is clear that the particle shows close paths for different densities at this time, which is much different from the case with the original drag. Also, the particle goes up more sharply for lower density instead of higher density as in original case. These imply that the small drags make the Saffman lift contribute more in the motion of the particle.

Above results are same as that in the case without considering the wall effect except for that larger density is required for the Saffman lift force to affect the motion of particles more significantly.

5. Conclusion

In this report, we introduced wall effect, which usually increases the drag force and decreases the Saffman lift force, into the model for particles moving in a slider/disk interface. Using this modified model, we studied the characteristics of small particles in an interface, which can be simplified as a 2-D case because the Saffman lift force has few effects on the motion of them. The simulation results show that density and initial velocities do not affect the paths of small particles significantly, and the small particles follow the streams very well. These results are similar to the cases without considering the wall effects.

We also studied the characteristics of large particles moving in a recessed region. The simulation results show that Saffman lift force shows more significant effect on the motion of particles with larger diameter, density and initial velocities. This conclusion is similar to the cases without considering the wall effect, except for the fact that larger diameter, density and initial velocities, compared to the cases without considering the wall effects, are required for the

Saffman lift force to show a significant effects on the motion of them, because wall effect usually reduces the magnitude of the Saffman lift force.

References

Brenner, H., 1961, “Effect of Finite Boundaries on the Stokes Resistance of An Arbitrary Particle”, *Chem. Eng. Sci.*, 16, pp 242.

Cha, E.T., Bogy, D.B., 1995, "A Numerical Scheme for Static and Dynamic Simulation of Subambient Pressure Shaped Rail Sliders", *ASME Journal of Tribology*, Vol. 117, pp.36-46

Chen, M., McLaughlin, J.B., 1995, "A New Correlation for The Aerosol Deposition Rate in Vertical Ducts", *Journal of Colloid and Interface Science*, 169, pp.437-455.

Drew, D.A., 1988, "The Lift Force on a Small Sphere in the Presence of a Wall", *Chemical Engineering Science*, Vol. 43, No. 4, pp. 769-773.

Faxen, H., 1923, Arkiv. Mat. Astro. Fys. 17, No. 8, *Dissertation*, Uppsala Univ.

Golaman, A.J., Cox, R.G., Brenner, H., 1967, "Slow Viscous Motion of A Sphere Parallel to A Plane Wall -I: Motion through a Quiescent Fluid", *Chemical Engineering Science*, Vol. 22, pp.637-651.

Kallio, G.A., 1989, "Wall-impact Velocities of Particles in The Turbulent Boundary Layer", *3rd International Symposium of Gas-Solid Flows*, ASME FED-Vol. 78, pp.1-5.

Liu, V.C., Pang, S.C., Jew, H., 1965, “Sphere Grad in Flows of Almost-Free Molecules”, *The Physics of Fluids*, Vol. 8, No. 5, pp. 788-796.

Lu, S., Bogy, D.B., 1994, "A Multi-Grid Control Volume Method for the Simulation of Arbitrarily Shaped Slider Air Bearing with Multiple Recess Levels", *CML report*, No. 94-016, UC Berkeley.

Lu, S., Bogy, D.B., 1995, "CML Air Bearing Design Program User's Manual", *CML report*, No. 95-003, UC Berkeley.

McLaughlin, J.B., 1993, "The Lift on a Small Sphere in Wall-bounded Linear Shear Flows", *Journal of Fluid Mechanics*, Vol. 246, pp. 249-265.

O'Neill, M.E., 1965, "A Slow Motion of Viscous Liquid Caused By A Slowly Moving Solid Sphere", *Mathematika* 11, pp. 67-74

Partanka, S.V., 1980, "Numerical Heat Transfer and Fluid Flow", *Hemisphere Publishing Corporation*.

Saffman, P.G., (1965), "The Lift on A Small Sphere in A Slow Shear Flow", *Journal of Fluid Mechanics*, Vol. 22, part 2, pp. 385-400.

Saffman, P.G., (1968), " The Lift on A Small Sphere in A Slow Shear Flow (Corrigendum)", *Journal of Fluid Mechanics*

Schaaf, A.L., Chambre, P.L., 1961, “Flow of Rarefied Gases”, *Princeton University Press*.

Shyy, W., Sun, C.S., 1993, "Development of A pressure-correction/Staggered-grid Based Multi-grid Solver for Incompressible Recirculating Flows", *Computer and Fluids*, Vol. 22, No. 1, pp.51-76.

Wakiya, S.J., 1957, “Viscous Flows past A Spheroid”, *Journal of the Physical Society of Japan*, Vol. 12, No. 10, pp 1130-1141.

Wakiya, S.J., (1960), *Res. Rep. Fac. Eng. Niigata Univ.*, (Japan) 9, 31.

Zhang, S., Bogy, D.B., 1996, "Slider Designs for Controlling Particle Contamination", accepted to *1996 ASME/STLE Tribology Conference* and publishing in *Journal of Tribology*.

Zhang, S., Bogy, D.B., 1996b, Slider Designs for Controlling Particle Contamination: Case Study", *CML Report*, No. 96-012

Zhang, S., Bogy, D.B., 1996, "Effects of Lift on the Motion of Particles in the Recessed Regions of a Slider", submitted to the Physics of Fluids.

Table 1. Flying Characteristics: Slider #1

Position *r* (*mm*)	Skew (degree)	Pitch (μ rad)	Roll (μ rad)	FH-CTE (*nm*)
23	0.0°	188.2	0.0	34.2

Table 2. Flying Characteristics: Slider #2

Position *r* (*mm*)	Skew (degree)	Pitch (μ rad)	Roll (μ rad)	FH-CTE (*nm*)
23	0.0°	266.4	8.9	31.3

Table 3. Flying Characteristics: Slider #2 at ID and OD

Position *r* (*mm*)	Skew (degree)	Pitch (μ rad)	Roll (μ rad)	FH-CTE (*nm*)
15	-7.5°	475.5	9.8	40.8
31	7.5°	98.4	6.5	20.1

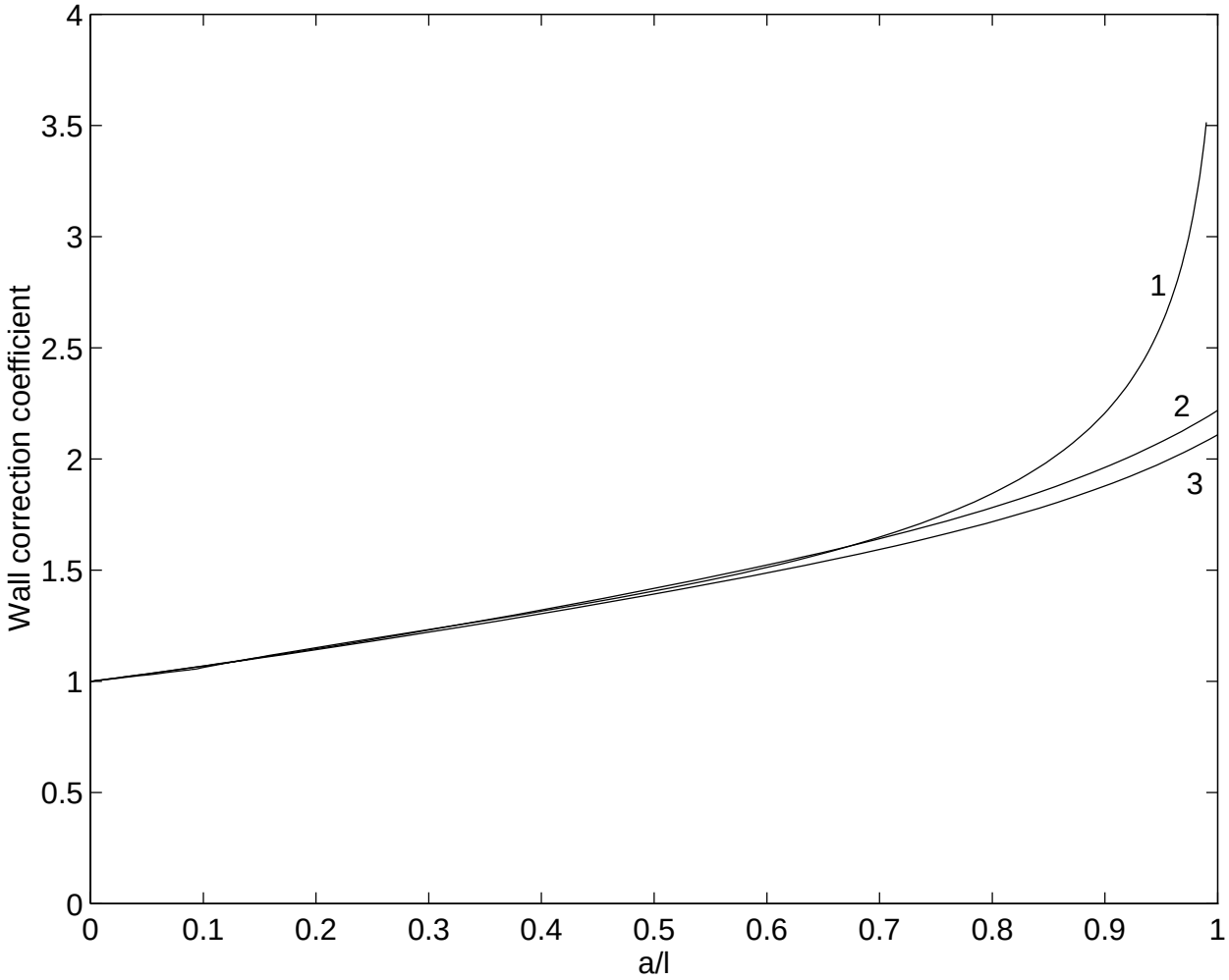

Fig. 1 Comparison of wall effect coefficiets: 1-- Chen et al's; 2-- Wakiya's, Poiseulle flow; 3-- Wakiya's, Couette flow

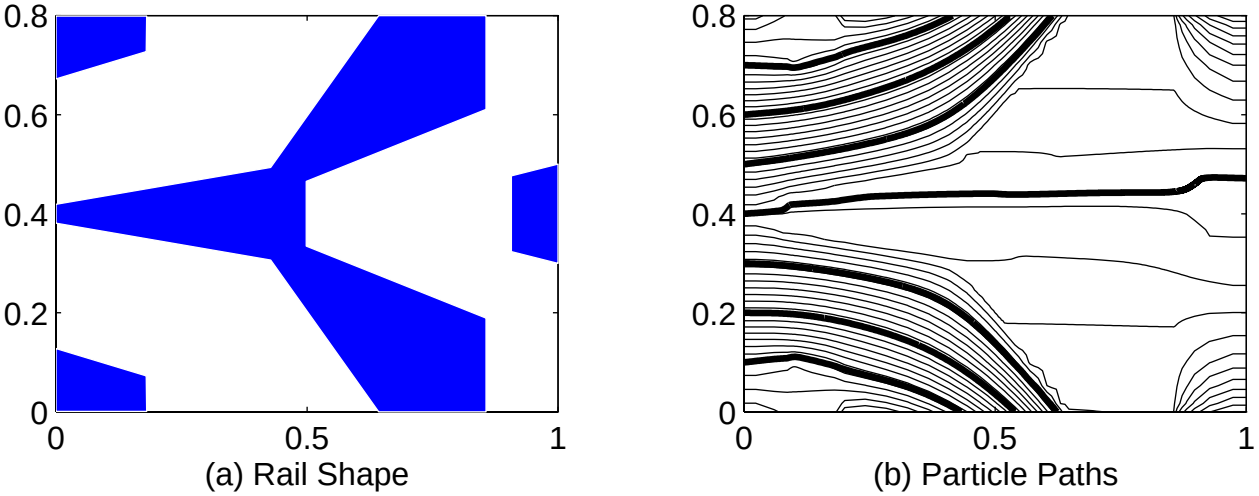

Fig. 2 Particle paths for slider #1

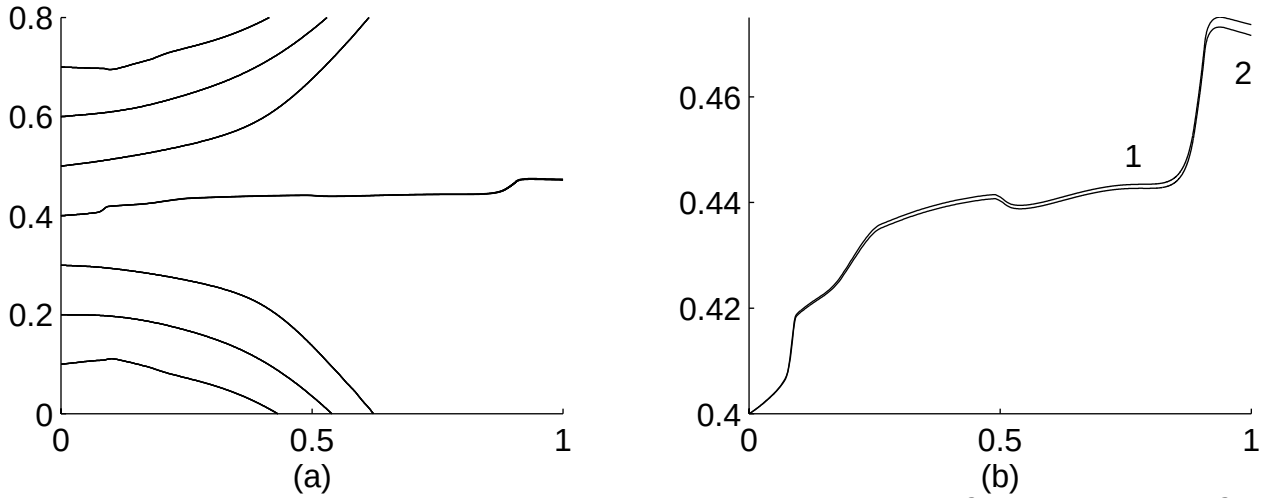

Fig. 3 Effects of particle density on the particle paths: 1-- ρ_p=1000 kg/m^3; 2-- ρ_p=8000 kg/m^3

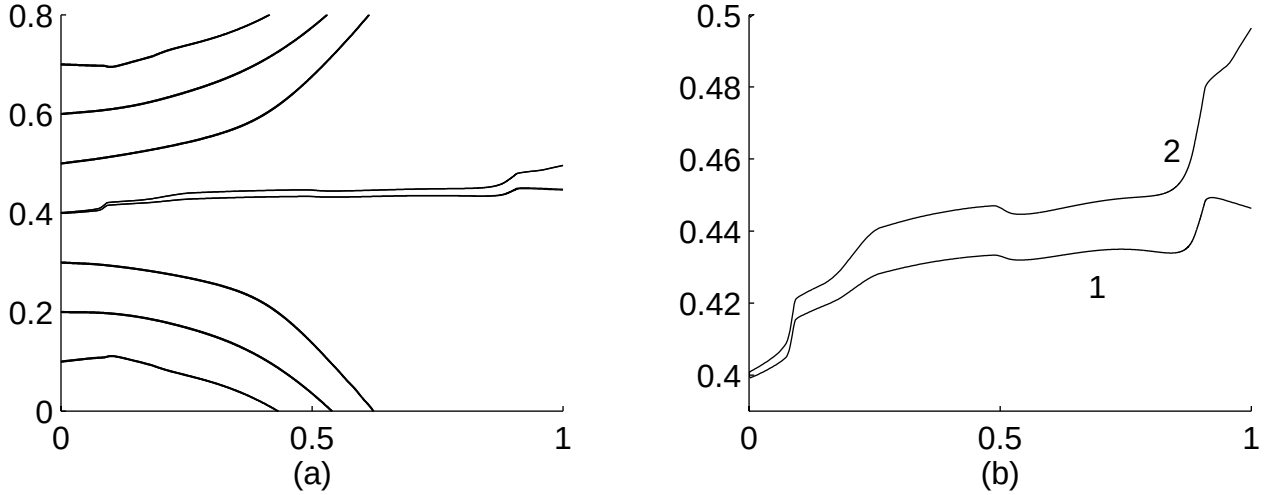

Fig. 4 Effects of initial velocities on the particle paths: 1-- (U_0,V_0)=(1,-1); 2-- (U_0,V_0)=(0,1).

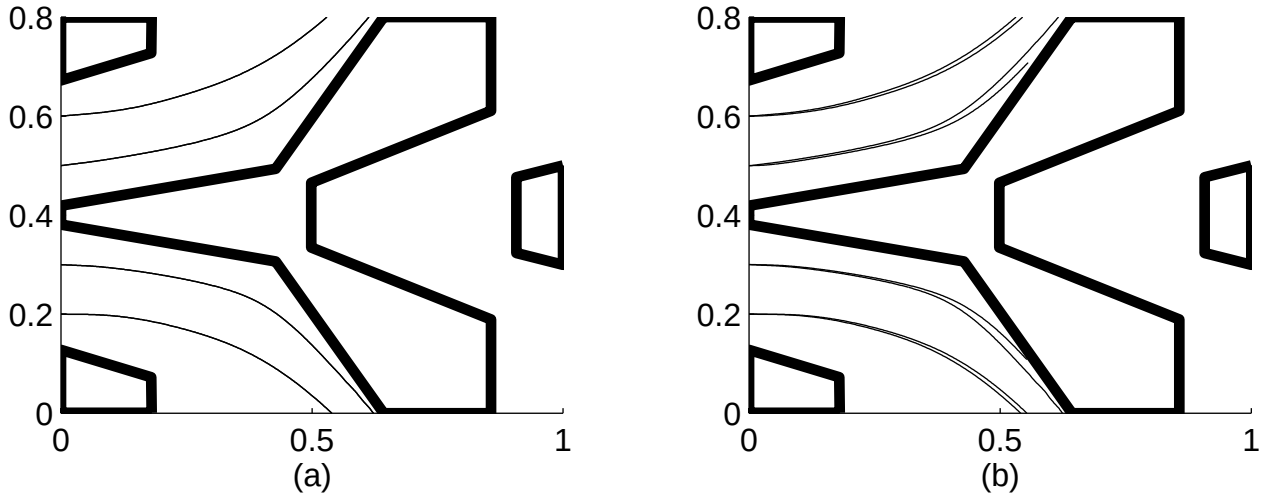

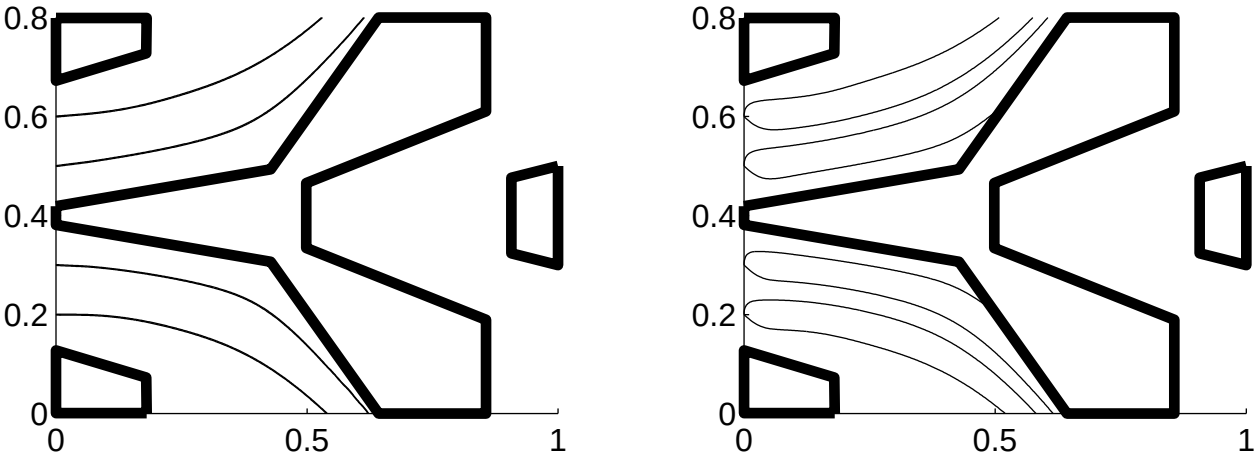

Fig. 5 Effects of particle density and initial velocities on the particle paths under different particle sizes

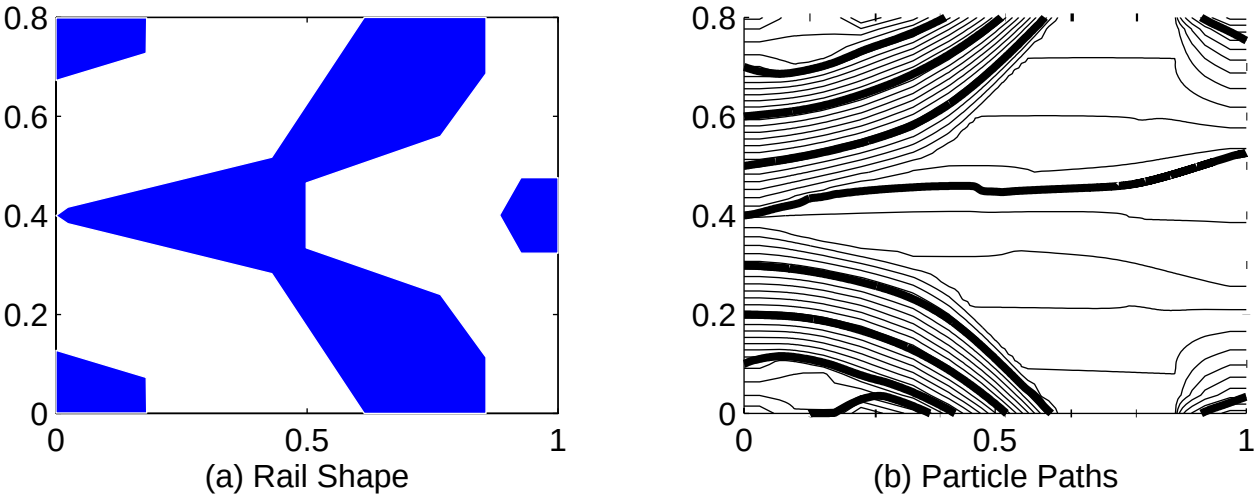

Fig. 6 Particle paths for slider #2

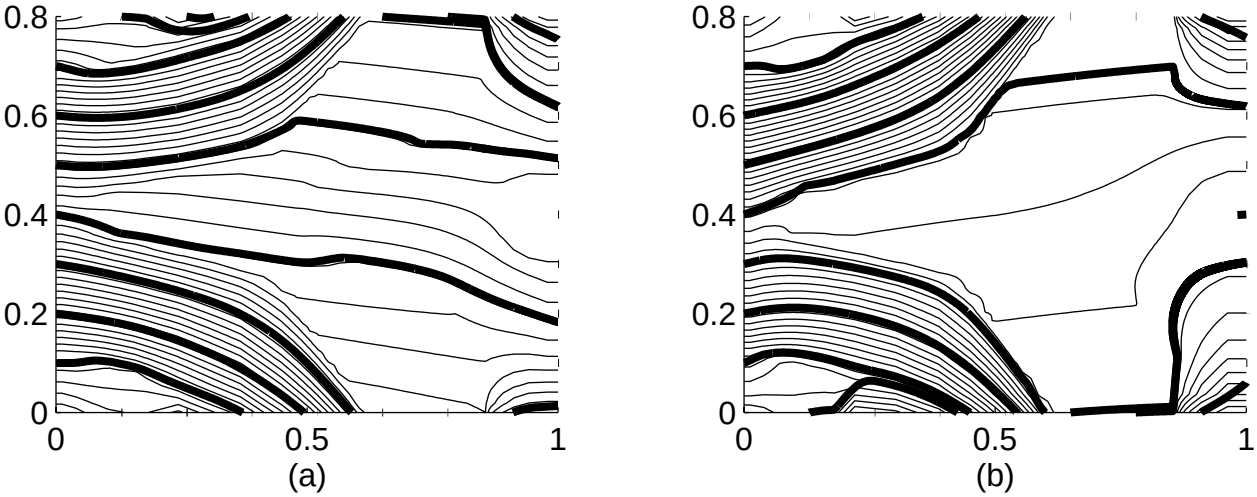

Fig. 7 Particle paths for slider #2 at ID (a) and OD (b)

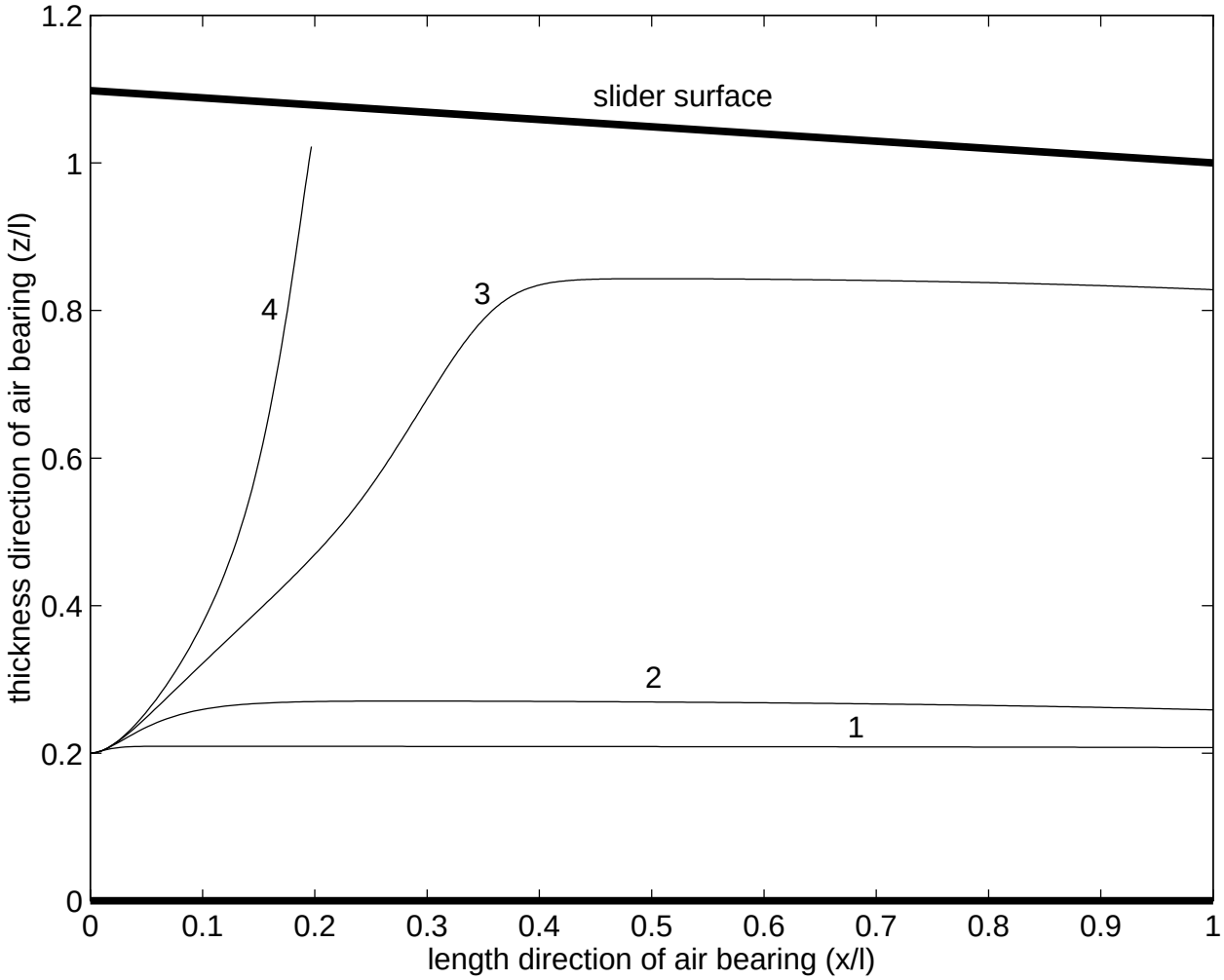

Fig. 8 Effects of particle diameter on the particle motion: 1-- *d*=200 *nm*; 2-- *d*=300 *nm*; 3-- *d*=330 *nm*; 4-- *d*=340 *nm*.

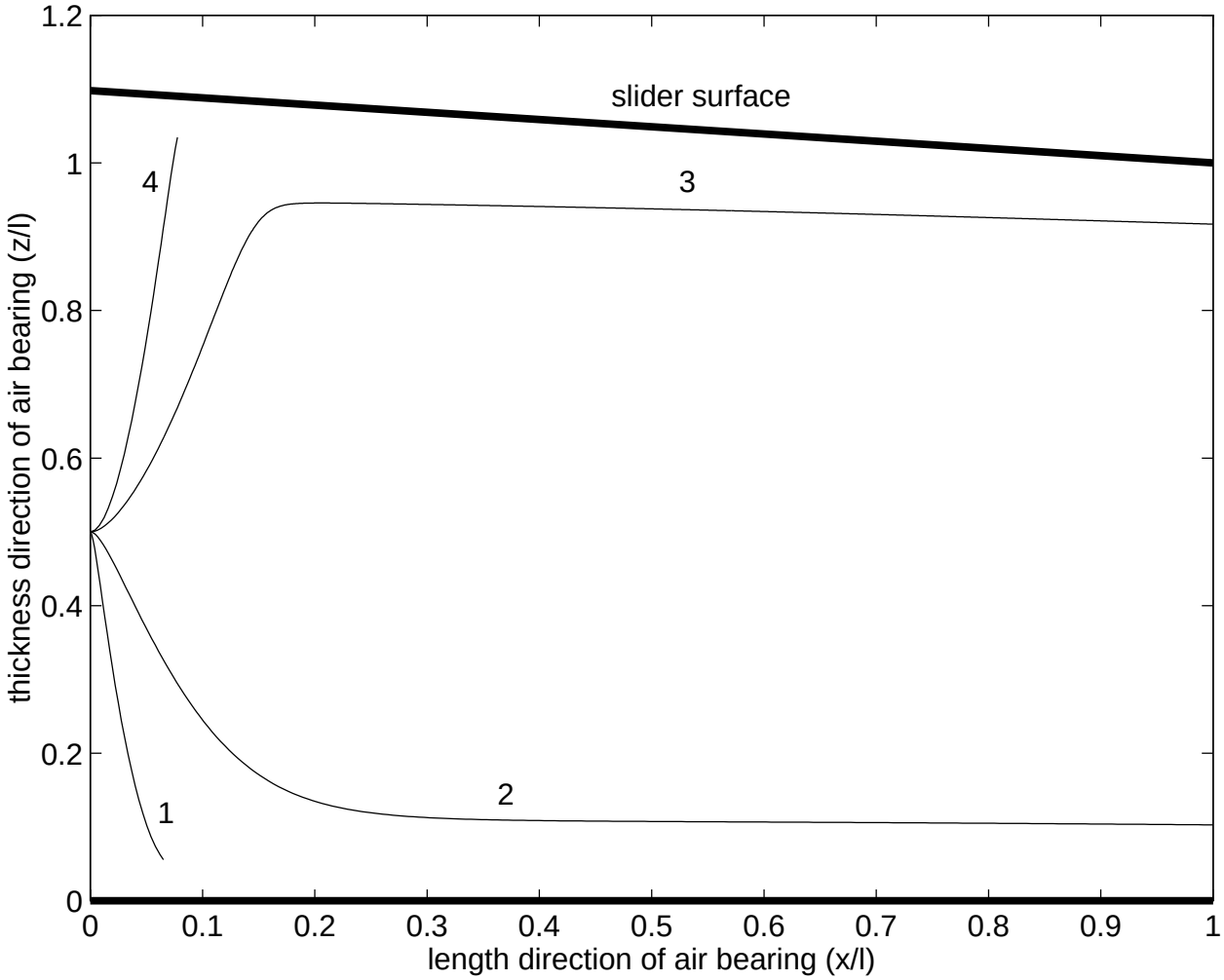

Fig. 9 Effects of initial velocities on the particle motion: 1-- U_0=0.2; 2-- U_0=0.4; 3-- U_0=0.6; 4-- U_0=0.8.

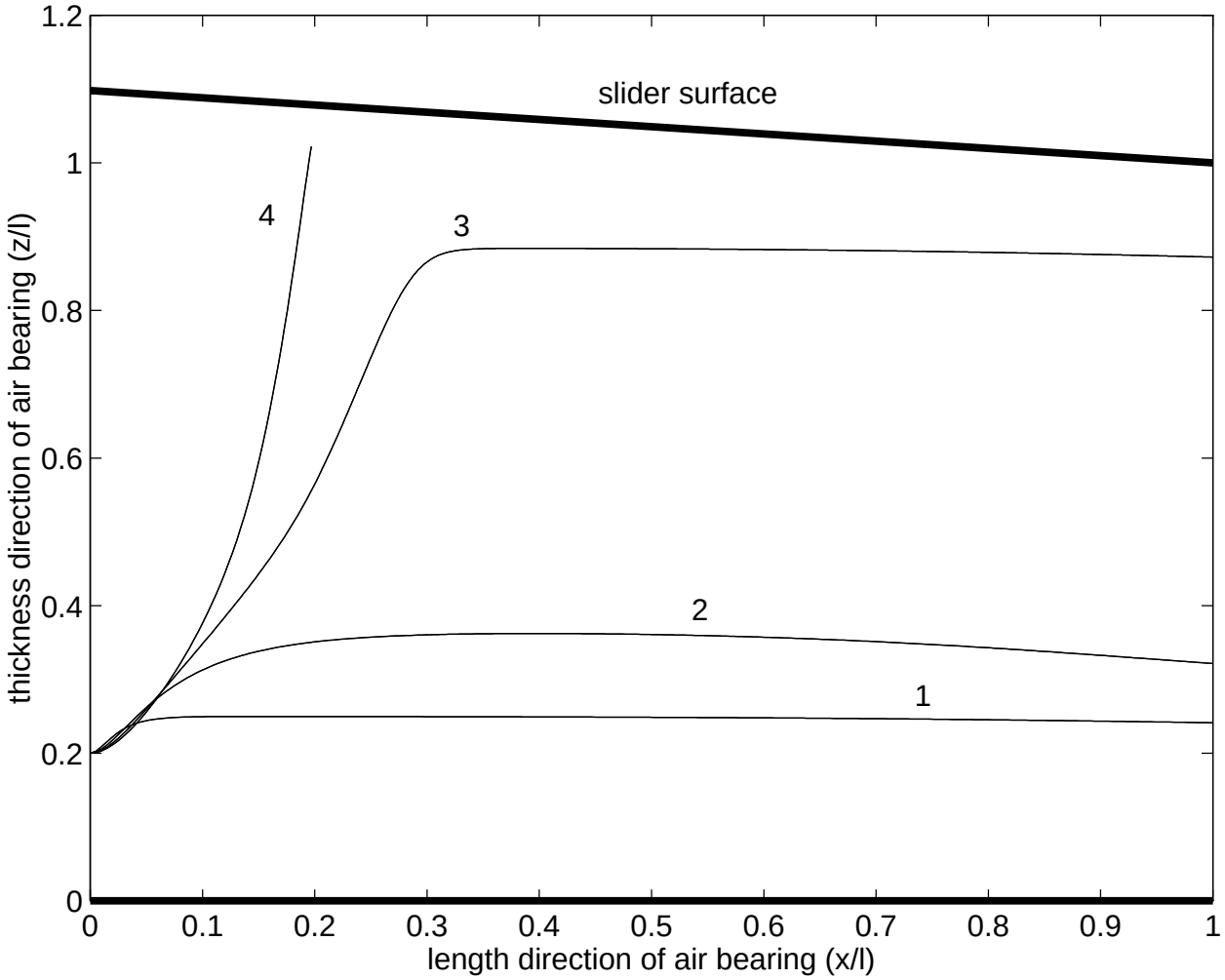

Fig. 10 Effects of particle density on the particle motion: 1-- ρ_p=2000 kg/m^3; 2-- ρ_p=4000 kg/m^3; 3-- ρ_p=6000 kg/m^3; 4-- ρ_p=8000 kg/m^3.

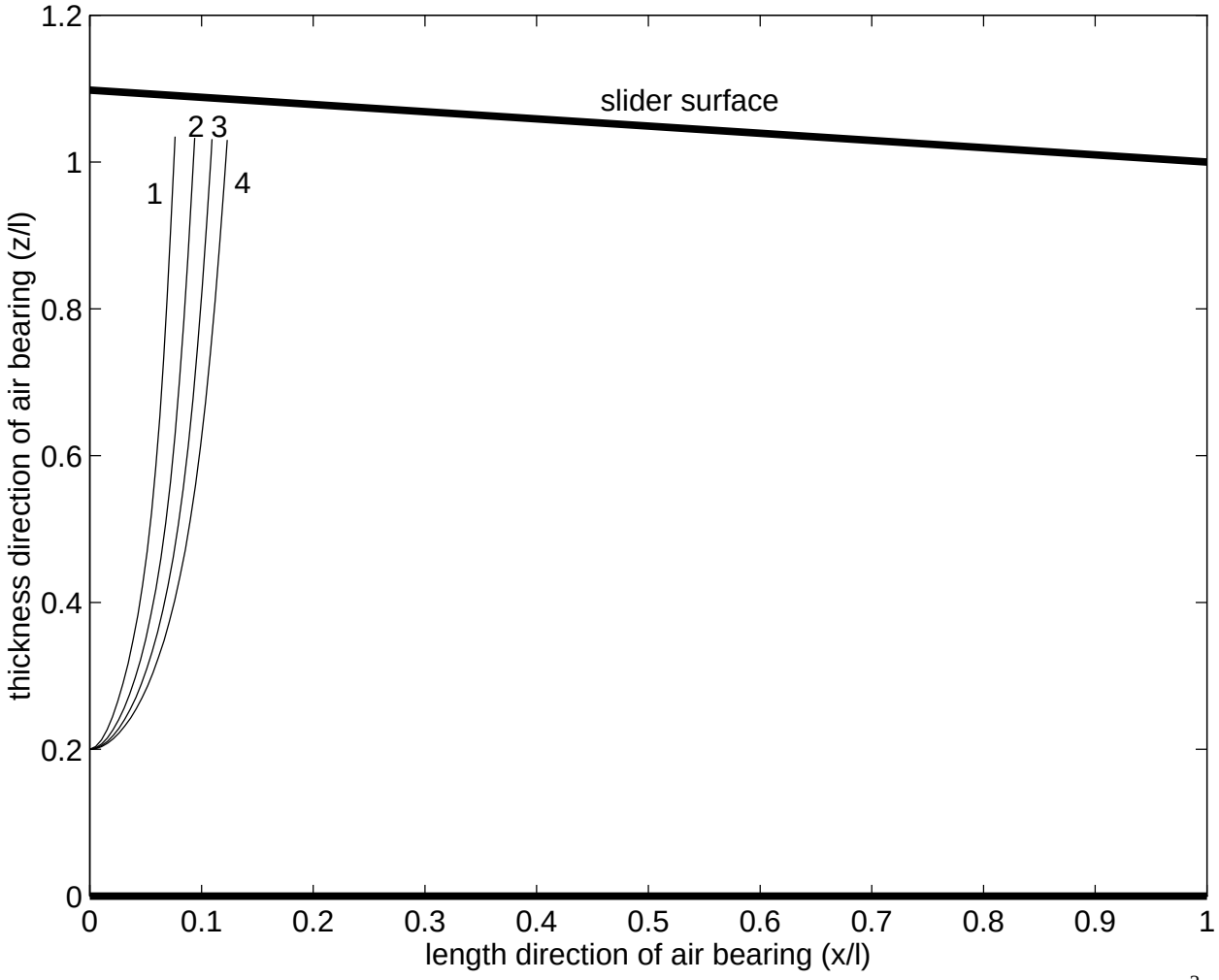

Fig. 11 Effects of particle density on the particle motion (1/3 reduced drag): 1-- ρ_p=2000 kg/m^3; 2-- ρ_p=4000 kg/m^3; 3-- ρ_p=6000 kg/m^3; 4-- ρ_p=8000 kg/m^3